The Effects of Large Ionospheric Gradients on Single Frequency Airborne Smoothing Filters for WAAS and LAAS

Todd Walter, Seebany Datta-Barua, Juan Blanch, and Per Enge, *Stanford University*,

ABSTRACT

Both WAAS and LAAS receivers use carrier-smoothing filters to reduce the effects of multipath and thermal noise at the aircraft. For the majority of users this reduces the magnitude of the errors and leads to improved accuracy. However, the presence of a significant ionospheric gradient can introduce a bias into the output of this filter. If unmitigated, this bias can grow to be significantly larger than the noise and multipath effects the filter is employed to reduce. Such gradients are rare at mid-latitudes; however, they are much more common in polar-regions and sometimes a daily occurrence in equatorial regions. Therefore, this problem which may be rare in the United States or Europe will be much more significant in other parts of the world.

The bias arises because the GPS code and carrier measurements are affected differently by the ionosphere. A positive delay for the code creates an equal, but opposite advance for the carrier. Therefore, as the ionospheric Total Electron Content (TEC) changes along a user's line of sight to the satellite, the code and carrier measurements diverge from each other at twice the rate of ionospheric change. Nominally, the rate of change over a few hundred seconds is very small (less than a few millimeters per second) leading to decimeter-sized biases or less. However, if the user's line of sight traverses a significant ionospheric gradient, the TEC can change by tens of meters in just a few minutes. This in turn can create a biased filter estimate of greater than 20 meters. This error is large compared to the overall error budget less than 0.4 m one-sigma.

This paper investigates the combined effect of the TEC change and the filter bias on the WAAS/LAAS user's differential range error and suggests a remedy to lessen the impact. This solution includes changes to the airborne algorithms to detect large differences between the code and carrier. The ability of the airborne receiver to detect this bias depends on the amount of thermal noise and multipath it experiences. This paper will review the current expected levels of noise and multipath and indicate level of performance that should be achievable.

INTRODUCTION

The concept of carrier smoothing dates back to the early 1980's [1]. The idea is very clever: use the noisy code measurements to estimate the bias on the comparatively quiet carrier measurements. Thus, we take the best of each, the absolute measurement of the code and the low noise of the carrier (see Figure 1 for an example of the smoothing process). This works exceptionally well because the code and carrier are identically affected by the time-of-travel between the satellite and the user, and by each of their clocks. These terms are by far the largest in the two measurements. Unfortunately, the code and carrier are not affected identically by the ionosphere. The code is delayed by an amount proportional to the Total Electron Content (TEC) along the line of sight from the satellite to the user. The carrier, however, is advanced by nearly the same amount [2]. Thus, the effect on each is nearly equal and opposite.

Fortunately, for the Conterminal United States (CONUS), the ionosphere normally is slowly varying. Therefore, for short smoothing times, this difference can be incorporated into the estimate of the carrier bias and the resulting error is negligible. However, there are times when the ionosphere may change by a large amount in a comparatively short time. These events are rare in CONUS, but are more common in other parts of the world, particularly in equatorial regions [3]. These rapid changes can introduce significant error to the smoothing process. For very large variations, the error can be significantly larger than the multipath errors the smoothing is intended to mitigate. Figure 2 provides an example of the effects of a small rate of change in the ionosphere. Here the output of the smoothing filter is clearly biased slightly below the mean of the code measurements. To understand the cause of this effect we will look into the filter in detail.

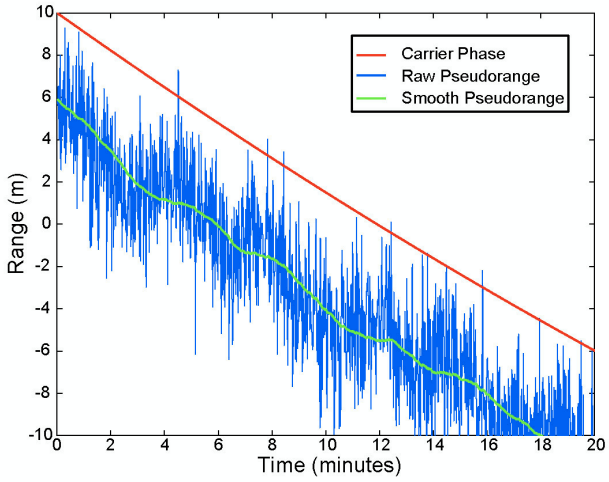

Figure 1. *The code measurements (blue) are absolute, but affected by noise while the carrier measurements (red) a virtually noise-free but biased. The smoothing filter combines them together to for the relatively unbiased and low-noise range estimate (green).*

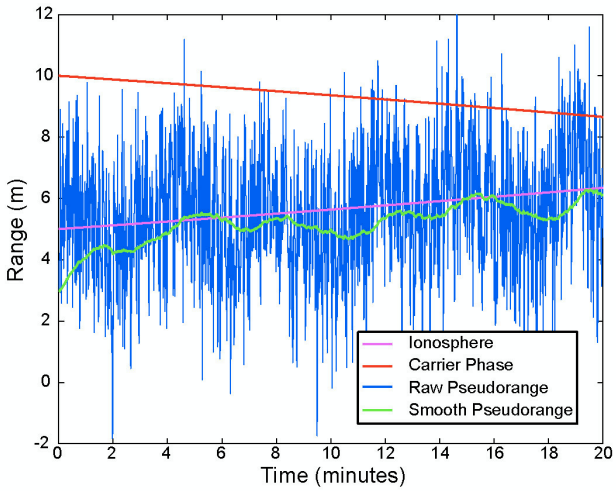

Figure 2. *A rate of change in the ionosphere (magenta) will cause a bias in the output of the smoothing filter.*

SMOOTHING EQUATIONS

Carrier smoothing of GPS measurements is a concept that is more than twenty years old. The equations are well known to most practitioners, but they still are worth repeating. The instantaneous pseudorange measurement at time t_i will be designated ρ_i and the corresponding phase measurement is ϕ_i. The smoothed pseudorange at time t_i is designated S_i and is given by

$$S_i = \frac{\rho_i + (k-1)\cdot(S_{i-1} + \phi_i - \phi_{i-1})}{k} \qquad (1)$$

Here we can see that the smoothing estimate from the prior epoch, S_{i-1}, is forward propagated using the carrier measurements and averaged with the current pseudorange measurement. The propagated term is given more weight; here k represents the amount of smoothing. Larger values indicate a greater amount of smoothing with an associated longer time constant.

We can investigate the effects of carrier smoothing in more detail by identifying key components of the code and carrier measurements

$$\begin{aligned} \rho_i &= r_i + I_i + M_i \\ \phi_i &= r_i - I_i + b \end{aligned} \qquad (2)$$

Here r_i represents common mode terms such as the range to the satellite, clock offsets, and tropospheric delay, I_i is the ionospheric delay/advance, M_i is the code multipath and b is the carrier bias. Substituting these values into (1) and subtracting $r_i + I_i$ from both sides yields the error in the smoothed value ($\varepsilon_i \equiv S_i - r_i - I_i$) as a function of time

$$\varepsilon_i = \frac{(k-1)\cdot(\varepsilon_{i-1}) - 2(k-1)\cdot(I_i - I_{i-1}) + M_i}{k} \qquad (3)$$

With a little rearranging, the above equation can be approximated by a continuous expression

$$\frac{\partial \varepsilon}{\partial t} = -\frac{\varepsilon}{\tau} - 2\frac{\partial I}{\partial t} + \frac{M}{\tau} \qquad (4)$$

Where $\tau = (k - 1)(\Delta t)$ is the smoothing time constant. This is a first order linear differential equation whose solution is given by

$$\varepsilon = e^{-\frac{t}{\tau}}\left[\varepsilon_0 - \int_{t'=0}^{t} e^{\frac{t'}{\tau}} \cdot \left(2\frac{\partial I}{\partial t'} - \frac{M}{\tau}\right) dt'\right] \qquad (5)$$

Now we have a non-iterative expression for the error in the smoothing filter as a function of the ionospheric delay and multipath.

To see the effect of multipath on the filter, let us examine the case with no ionospheric change. We set the ionospheric divergence term to zero and ignore the initial value to obtain

$$\varepsilon = e^{-\frac{t}{\tau}} \left[\int_{t'=0}^{t} e^{\frac{t'}{\tau}} \cdot \frac{M(t')}{\tau} \, dt' \right] \quad (6)$$

We will examine two extremes: a constant bias and white noise. If the multipath has a very long period compared to τ, then it is effectively a constant term in the integral. The resulting error term equals the constant multipath. Thus, the smoothing filter is completely ineffective against long-period multipath. If the multipath is modeled as uncorrelated, zero-mean, white noise, then the expected value of the error will be zero while the expected variance of the error will the variance of the multipath divided by $2(k - 1)$.

Actual multipath typically falls somewhere between these two models. There is some time correlation, which for airborne users should be less than the 100-second time constant. Thus, in absence of ionospheric variations, longer time constants lead to smaller errors. However, as we will see in the next sections, rapid rates of change in the ionosphere limit the performance of these filters.

IONOSPHERIC RATE OF CHANGE

As we can see from the equations from the previous section, the error in the smoothing filter depends very strongly on the rate of ionospheric variation. When we model the ionosphere as having a constant slope, we can evaluate the integral explicitly

$$I = a \cdot t$$

$$\frac{\partial I}{\partial t} = a$$

$$\varepsilon = e^{-\frac{t}{\tau}} \left[\varepsilon_0 - 2 \int_{t=0}^{t} e^{\frac{t}{\tau}} \cdot a \, dt \right] \quad (7)$$

$$\varepsilon = e^{-\frac{t}{\tau}} \left[\varepsilon_0 - 2a \cdot \tau \cdot e^{\frac{t}{\tau}} \right]_{t=0}^{t}$$

$$\varepsilon = \varepsilon_0 \cdot e^{-\frac{t}{\tau}} - 2a \cdot \tau \cdot \left[1 - e^{-\frac{t}{\tau}} \right]$$

This shows that any initial offset decays to zero while the filter error asymptotically approaches a constant offset equal to negative two times the rate of change, times the time constant. For example, a rate of change of +10 mm/second would approach a –2 m error in a filter with a 100-second time constant. Of course, for the error to come close to the limit, the rate of change would have to be sustained for several time constants.

IONOSPHERIC OBSERVATIONS

It is important to determine the typical and extreme behaviors of the ionosphere so we can determine the expected error in the smoothing filter for each case. It is well known that the ionospheric activity follows an 11-year cycle linked to solar activity [2]. Therefore, we expect typical days during the minimum period to have smaller rates of ionospheric change than during the solar maximum period. The most recent solar peak occurred during the year 2001 and activity was high for the surrounding years.

We have analyzed a typical day from 2000 that would correspond to high solar activity, but is devoid of any disturbances in the CONUS ionosphere. The day chosen was July 2, 2000. We investigated the nearly noise-free carrier phase data from the 25 WAAS Reference Stations (WRSs) [4]. Each WRS provides measurements at L1 and L2. By looking at the carrier phase differences between the two frequencies, we can determine the rates of change of the ionosphere over the specific lines of sight. We looked at measurements spaced apart by 100-second intervals. Thus, we investigated the average rate of change over a 100-second period.

Figure 3 shows a histogram of the data. As expected, the average value is very close to zero. The remainder of the data is bounded by eight mm/s and the majority is below one mm/s. Thus, one mm/s is a good typical number and eight mm/s is a good bound for a typical day. This leads to a maximum error of 1.6 m for a 100 second filter.

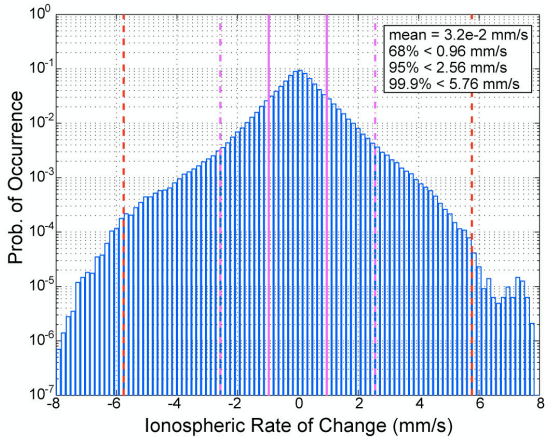

Figure 3. *A histogram of rates of TEC change for a quiet solar maximum day. The data is bounded eight mm/s. Days with ionospheric disturbances can have significantly larger values.*

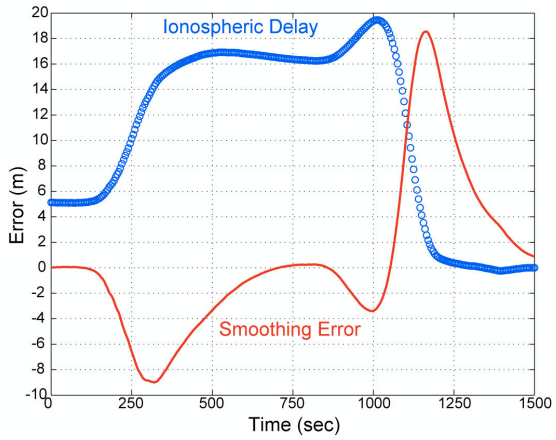

Figure 4. *The ionospheric delay from PRN 11 to a receiver in Virginia is shown during the ionospheric disturbance of October 29, 2003. The rapid rate of change of greater than 150 mm/s is evident. The red line shows the corresponding smoothing filter error (Data provided by Karl Shallberg of Zeta Associates).*

Unfortunately, there are ionospheric disturbances that can create significantly larger rates of change [5]. It is an open question just how large such gradients can become. The largest known event to date was observed by a receiver in Virginia during a severe ionospheric disturbance on October 29, 2003. The observation to PRN 11 by a dual frequency receiver had a change in its slant ionospheric delay of nearly 15 meters over a 100 second interval. Figure 4 shows the time history of the ionospheric delay (with an arbitrary offset). Also shown is the resulting 100-second smoothing filter error. The filter does not hit its theoretical limit of 30 m because the gradient only lasted for a little longer than one time constant. Other locations had similarly large values on this day: PRN 28 saw a nine-meter change over 100 seconds at Billings Montana, as did PRN 7 at Seattle.

These rapid changes in slant ionosphere appear to result from the motion of the IPP in relation to a sharp spatial gradient. The specific observation to PRN 11 had an elevation angle of about 30 degrees. It is conceivable that had the gradient passed through at a different time or had there been a satellite in the right place lower in the sky, there might have been an even greater ionospheric change from the same feature. Thus, it is difficult to establish just how large such rates of change may become. Instead, we should be focusing on what we can do to identifying such effects and how they may be prevented from causing harm to the user.

USER ERROR

A 150 mm/s sustained rate of change could give rise to a 30 m error in the airborne smoothing filter. The total airborne error component for WAAS is to be bounded by 35 cm 1-sigma value. Therefore, if left undetected, we could have an 85-sigma error in the range domain. Such features are also protected by the GIVE. For WAAS, gradients much greater than 10 mm/s are only observed during storms. During these events, the GIVEs are set to 45 m (13.7 m 1-sigma bound) [6]. Thus, the total error is protected. However, it is desirable to be less conservative during storms to gain availability for all but the very worst part of the most disturbed days. First, we must address the concern over missing a feature that may be sampled by the user receiver, but by none of the ground reference stations [7]. One such method may be to implement some form of airborne monitoring.

For LAAS the situation is different, because the aircraft and reference station are very close together and using identical smoothing filters, most of the error cancels. However, two concerns remain. First, the two are not exactly co-located, so steep spatial gradients will lead to significant differences [5][8]. Second, a cycle slip on one filter and not the other can lead to a significant difference during a rapid temporal gradient. In the first instance, the relevant characterization of the ionospheric gradient is not in terms of mm/second, but rather mm/km combined with the velocity of the IPP relative to the gradient. These latter two values are more difficult to determine, as they require a network of very closely spaced receivers to fully separate the values. Much work has been performed to try to understand the range of possible values, but once again, the focus should be on limiting the impact of such a threat to the user. Here too airborne monitoring may be the best approach.

AIRBORNE MONITOR

The aircraft is at a disadvantage because it only has single frequency measurements made from a dynamic platform. It cannot use dual-frequency information, as can the WAAS reference stations. However, it has the only direct measurements specific to the exact aircraft location. Because the ionosphere affects the code and carrier differently, we can use those differences as the basis for direct airborne monitoring. This will avoid the uncertainty of the ground experiencing different ionosphere than the aircraft. Here the affected measurements are used directly.

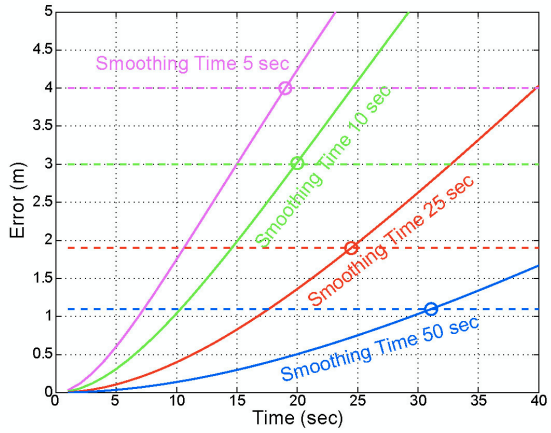

Figure 5. *The difference between a 100-second filter and four shorter filters is shown here in response to a 150mm/s ionospheric rate of change. Although the longer filters have less noise and lower thresholds, the shorter filters are the quickest to cross their thresholds*

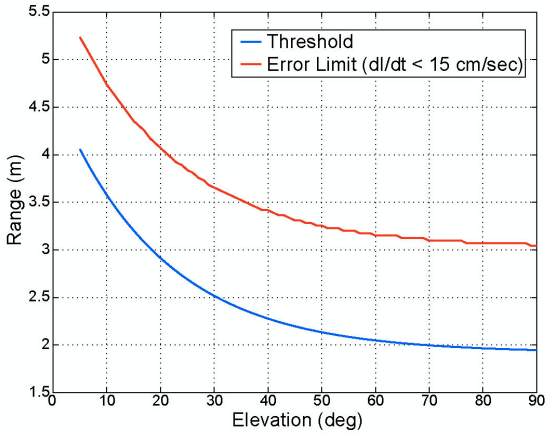

Figure 6. *An example threshold (blue) and the corresponding maximum undetected error on the 100-second filter are shown using a five second filter for comparison.*

The LAAS and WAAS MOPS specify a standard 100-second smoothing filter [9]. Perhaps another filter with a different time constant would make a good comparison. If the filters disagree by more than a certain amount, it could be an indication of a rapid rate of change. Equation (7) provides the formula for the rate of error growth in the filter in response to a constant gradient. A filter with a much shorter time constant would appear to have the most different response to the gradient. It would settle into a smaller bias and do so faster. However, shorter time-constants lead to noisier outputs. Thus, the threshold we would compare against would have to increase. There is an optimal time constant that will provide the fastest time-to-detect. Unfortunately, this optimal value will depend on the characteristics of the multipath and noise, it may be different for different installations, and may even vary over time.

Figure 5 shows the rate of growth in the difference between the 100-second filter and four shorter ones. The ionospheric gradient has been set to 150 mm/s. The thresholds were derived from simulated multipath. The details of this simulated multipath will be presented in the next section. The thresholds have been set to keep the false alarm rate low. The true threshold values depend very strongly on the real multipath characteristics. A high margin is desirable to prevent taking drastic action on small rates of change. The multipath model used in this paper is a rough approximation. Exact threshold determination requires higher fidelity models of the airborne environment.

As the figure indicates, longer smoothing time constants have less noise and lower thresholds. However, despite the higher noise and larger thresholds, the shorter smoothing times trigger faster and thus yield smaller undetected errors. We recommend comparing the 100-second filter to a filter with a time constant of 10 seconds or less.

When the difference between the 100-second filter and the shorter filter crosses the threshold, the satellite should be removed from the solution or severely deweighted. The fourth note of Section 2.1.4.1.2 of the WAAS MOPS states this already should be the action for large successive disagreements between the raw code and smoothed code [9]. However, the threshold is very large (10 m) and the definition of successive is vague. Worse, it recommends not updating the smoothing filter with the raw pseudorange for the first few instances of this condition. While this is an appropriate response to multipath or interference, it makes the ionospheric divergence problem even worse! We agree with this course of action in general, but feel that successive observations should be limited to no more than two or three seconds.

When the shorter filter and/or the raw pseudorange measurement are in disagreement with the 100-second filter, it indicates an inconsistency between the code and carrier measurements. There are many possible causes including multipath, ionospheric gradients, and interference. Which measurement to trust more depends on the cause. Thus, the best course of action cannot be determined without more information. Since that

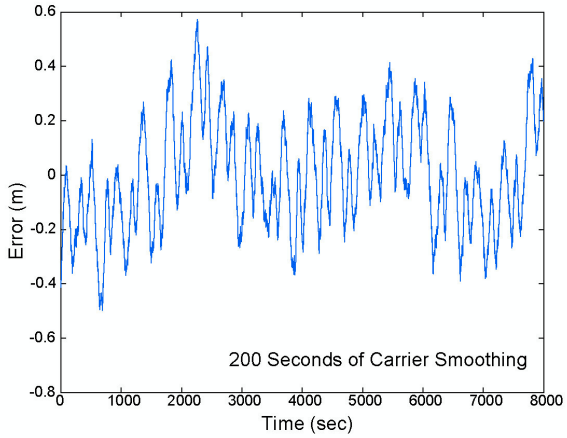

Figure 7. *A sample plot of the simulated multipath put through a 200 second smoothing filter.*

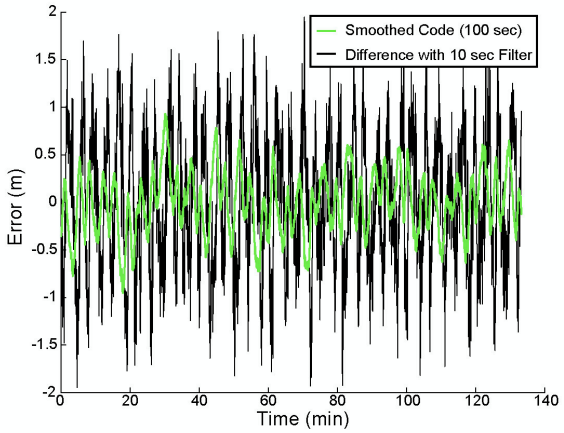

Figure 8. *The simulated multipath is run through a 100 second smoothing filter and its influence on the difference between the 100-second filter and a 10 second filter (black) is shown. It can be seen that the difference is always less than 2 m, which leads to the 3 m threshold in Figure 5.*

information is unavailable to the user, the safest course of action is to remove the satellite from the position solution or sufficiently deweight it. The satellite can be reintroduced when the measurements are back in agreement with each other.

The thresholds in Figure 5 are based on expected multipath at low elevation angles. An ionospheric event affecting a higher elevation angle will have smaller multipath and correspondingly smaller thresholds. Figure 6 shows an example threshold (blue) and the corresponding maximum undetected smoothing error in the 100-second filter (red) assuming an ionospheric gradient of 150 mm/s or less. Again, the thresholds provided here are for illustrative purposes only. To set the true threshold values requires greater knowledge of the airborne multipath characteristics.

Although it is not clear that 150 mm/s is the worst possible gradient, this approach does show that an airborne detector can prevent a potential 30 m error from growing larger than 5 m. This is a significant reduction and it could translate into a significant improvement in availability. For WAAS, the concern over protecting against unobserved ionospheric errors during storms forces the broadcast of very large GIVE values (15 or 45 m) [6][7]. If we could rely on airborne detection of all errors greater than 5 m, this would translate into a tremendous increase in vertical guidance availability during disturbed conditions. For LAAS the impact would be similar. If the air could be trusted to detect these steep temporal gradients (that in turn arise from steep spatial gradients), then the ground could allow the use of far more geometries. Currently, restricting availability to periods with truly robust geometries is one potential solution to this threat [8]. An airborne monitor addresses the problem much more directly and provides much higher availability.

AIRBORNE MULTIPATH

The simulated multipath used to determine the thresholds was based on data from operating aircraft. Multipath from an airborne, moving aircraft is different from what would be observed from a static airplane on the ground. Unfortunately, this limits our ability to collect large amounts of data. Previously the best description of airborne multipath characteristics came from a data collection campaign in the late 1990's [10]. Unfortunately, there are several limitations to this data. It was collected using a 200 second smoothing filter, so any information about the short-term multipath characteristics is lost. It is not possible to accurately reconstruct the behavior of a five second filter without making many assumptions. Additionally, the researchers on this project suspect that test set-up was not ideal and may have overestimated the true amount of multipath (see the post validation data analysis section in [10]).

In order to use the information from this study, a highly simplified multipath signal was simulated. It was adjusted to make the output of a 200 second smoothing filter similar in appearance to Figure 4 in [10]. The rather arbitrary formula selected was

$$M(t) = \left(1 + A_1 \cos(\omega_1 t)\right) \sin(\omega_2 t + \sin(\omega_3 t)) + N(0, \sigma_M) \quad (6)$$

Where we have assigned the values A_1 = 0.025 m, ω_1 = 0.0192 rad/s, ω_2 = 0.0295 rad/s, ω_3 = 0.0158 rad/s and ω_M = 2 m. The resulting 200-second smoothed value is shown in Figure 7. This should be compared to Figure 4 of [10]. Figure 8 shows the effect of the simulated multipath on a 100 second filter. Also shown is the corresponding difference between a 100 second filter and a 10 second filter. Here it can be seen that 3 m (as used in Figure 5) is a conservative threshold.

Fortunately, there is a new effort underway to better characterize the airborne multipath [11]. This new effort will address the shortcomings of the previous study by providing more accurate (and hopefully lower) multipath models and investigating the behavior over shorter times. The analysis of this new data should enable us to more accurately determine the real capabilities of airborne monitoring.

CONCLUSIONS

We have seen that ionospheric gradients exist and that they are capable of creating biases in the user-smoothing algorithm on the order of 20-30 m. We have shown that an airborne monitor utilizing the aircraft's single frequency code and carrier measurements can limit this error to five meters. Furthermore, this detector works directly on the ionosphere that the aircraft samples. It does not suffer from the ground monitoring limitation that it may be sampling different ionosphere.

More work needs to be performed to refine and verify the multipath model used. Proper thresholds must be determined and it must be demonstrated that the desired false alarm rates are achieved. However, airborne monitoring will be crucial to providing higher availability in the face of the large ionospheric gradients. This will prove to be particularly true in equatorial regions where significant gradients can be an everyday occurrence.

ACKNOWLEDGMENTS

The authors acknowledge the effort of Karl Shallberg of Zeta Associates in searching through WAAS data to find many of these ionospheric events and providing data to us. The work for this paper was supported by the FAA Satellite Product Team under research grant 95-G-005.

REFERENCES

[1] Hatch, R., "The Synergism of GPS Code and Carrier Measurements," in Proceeding of 3rd International Symposium on Satellite Doppler Positioning, Las Cruces, NM, 1982.

[2] Klobuchar, J. A, "Ionospheric Effects on GPS," in **Global Positioning System: Theory and Applications**, Parkinson & Spilker editors, AIAA, Washington, DC, 1996, pp. 485-516.

[3] Klobuchar, J., et al., "Ionospheric Issues for a SBAS in the Equatorial Region," in proceedings of the 10th International Ionospheric Effects Symposium, Alexandria, VA, May, 2002.

[4] Loh, R., et al., "The U. S. Wide-Area Augmentation System (WAAS)," in *NAVIGATION*: Journal of the ION, Vol. 42, No. 3, Fall, 1995

[5] Datta-Barua, S., Walter, T., Pullen, S., Luo, M., and Enge, P., "Using WAAS Ionospheric Data to Estimate LAAS Short Baseline Gradients," in Proceeding of ION NTM, San Diego, CA, January, 2002.

[6] Walter, T., et al. "Robust Detection of Ionospheric Irregularities," in NAVIGATION, Journal of the Institute of Navigation, vol. 48, no. 2, Summer 2001.

[7] Sparks, L., et al., "The WAAS Ionospheric Threat Model," in Proceedings of the International Beacon Satellite Symposium, Boston, June, 2001.

[8] Luo, M., et al., "Ionosphere Spatial Gradient Threat for LAAS: Mitigation and Tolerable Threat Space," in proceedings of National Technical Meeting of the ION, San Diego, CA, January, 2004.

[9] Minimum Operational Performance Standards (MOPS) for WAAS, RTCA document DO-229C

[10] Booth, J., et al., "Validation of the Airframe Multipath Error Allocation for Local Area Differential GPS," in proceedings of Annual Meeting of the ION, San Diego, CA, June, 2000.

[11] Murphy, T., et al., "Program for the Investigation of Airborne Multipath Errors," in proceedings of National Technical Meeting of the ION, San Diego, CA, January, 2004.